

Structure, Morphology and Conductive Properties of Sn-doped TiO₂

I.F. Mironyuk, T.R. Tatarchuk, V.O. Kotsyubynsky, V.I. Mandzyuk*, Kh.O. Savka, I.M. Mykytyn

Vasyl Stefanyk Precarpathian National University, 57, Shevchenko St., 76018 Ivano-Frankivsk, Ukraine

(Received 01 September 2020; revised manuscript received 15 December 2020; published online 25 December 2020)

The effect of Sn doping on the structure and morphology of Sn-doped TiO₂ samples has been investigated. The doped titania has been obtained by sol-gel synthesis using titanium aquacomplex precursor [Ti(OH)₂]₆³⁺·3Cl⁻ and SnCl₄ as a modifier. The structure and morphology of the samples have been studied through XRD analysis, TEM, low-temperature porometry, IR-spectroscopy, and EDS analysis. The conductivity of Sn-doped TiO₂ samples has been investigated by impedance spectroscopy. It was shown that the Sn-doped titania samples contain both anatase and rutile phases. The anatase/rutile ratio depends on the Sn content: the increasing Sn (IV) content from 3 to 12 % (wt.) leads to an increase in rutile content from 33.8 to 97.1 % (wt.). An increase in Sn content causes a decrease in the lattice parameter *a* and an increase in the parameter *c*. The presence of rod-shaped and needle-like rutile particles in the Sn-doped TiO₂ samples has been observed by TEM. The specific surface area for 6Sn/TiO₂ reached 290 m²/g. All the Sn-doped titania samples belong to the mesoporous materials. The mechanism of structure-forming processes is explained by existing Sn(OH)₄·2H₂O molecules in the reaction medium, which act as the centers of nucleation, growth and crystallization for rutile nanoparticles. The increase in Sn content leads to a decrease in the specific resistance of the studied materials compared to the undoped titania sample.

Keywords: Titania, Rutile, Anatase, Tin (IV) oxide, Specific conductivity.DOI: [10.21272/jnep.12\(6\).06024](https://doi.org/10.21272/jnep.12(6).06024)

PACS numbers: 61.43.Gt, 72.80.Tm, 81.20.Fw

1. INTRODUCTION

Anatase and rutile are crystal modifications of titanium dioxide, which have unique optical, adsorption and photocatalytic properties. They have a wide application in production of photonic functional materials [1], electrochromic film coatings [2], gas sensors [3], adsorbents for heavy metals extraction from an aqueous medium [4-7], etc. The phenomenon of photocatalytic decomposition of water on the TiO₂ surface has been discovered in 1972 by A. Fujishima and K. Honda [8]. This discovery gave impetus to an in-depth study of redox reactions involving photocatalysts. The formation of the electron-hole pairs (excitons) in the titanium dioxide lattice is possible under the light radiation. In this case, the formation of superoxide ions O₂⁻, and hydroxyl radicals HO·, HO₂· is observed. It allows to use the photocatalytic process to destroy the harmful organic substances in different environments, as well as for the synthesis of new organic compounds. Photocatalytic processes are used to neutralize toxic organic substances both in the aquatic environment and in the air [9]. The method of photocatalytic reduction of atmospheric carbon dioxide with the formation of methane or methanol is attractive to prevent the energy crisis and climate changes [10].

Currently, the anatase modification of titanium dioxide is more widely used as a photocatalyst compared to rutile modification. The known methods of TiO₂ synthesis are usually based on the sol-gel technology and give the anatase particles with a size less than 10 nm [11]. Other known methods (gas-phase method, template synthesis, hydrothermal and solvothermal methods) have the disadvantages: the rutile modification is usually obtained and the particle size exceeds 15-20 nm [12]. These technologies are expensive and require

high-cost equipment to be implemented. In order to obtain rutile with a small particle size, the sol-gel method is used and the metal cations (dopants) are introduced into the titanium precursor solution. This affects the crystallization process and ensures the rutile phase formation. In particular, the cations Sn (II), Cd (II), Fe (II), Ni (II), Mn (II), Zn (II), Co (II), Cr (II) and Cu (II) are promoters of rutile formation [13, 14]. The other double-charged cations with large ionic radii, such as Ca (II), Sr (II) and Ba (II) stabilize the anatase modification of titanium dioxide. Three-charged cations Al (III), Er (III), Y (III), Eu (III), Sm (III), Nb (III), La (III), four-charged cations Si (IV), Zr (IV), Se (IV), five-charged cations P (V), Nb (V) and six-charged cation S (VI) have also a stabilizing effect on anatase modification. The cations B (III) are an exception among the three-charged cations because they promote the rutile formation. The reason for rutile formation by low valence cations has been explained by the formation of oxygen vacancies in the TiO₂ structure [15].

The aim of this study is to determine the effect of Sn atoms on the crystal structure and morphology of the Sn-doped TiO₂ samples obtained by sol-gel synthesis. The titanium aquacomplex [Ti(OH)₂]₆³⁺·3Cl⁻ has been used as a precursor. The tin tetrachloride SnCl₄ has been used as a modifying agent. Such titanium aquacomplex showed its effectiveness in the synthesis of anatase adsorbents [4-6], which are effective in heavy metals removal from an aqueous medium. Usually four-charged metal cations stabilize the anatase modification. However, the modifying reagent SnCl₄ was chosen because the crystal structure of SnO₂ is the same as in the rutile (space group P4₂/mnm). Therefore, the isomorphic substitution of Ti atoms by Sn atoms should lead to the formation of a rutile modification of TiO₂. Since SnO₂ is an *n*-type semiconductor

* mandzyuk_vova@ukr.net

with a band gap of 3.3-3.6 eV [16], it is expedient to study the dependence of the Sn/TiO₂ samples conductivity versus the Sn content.

2. EXPERIMENTAL DETAILS

An appropriate amount of SnCl₄ solution was introduced into the solution of the titanium aquacomplex precursor [Ti(OH₂)₆]³⁺·3Cl⁻ in order to intercalate the Sn atoms into the crystal structure of TiO₂ during sol-gel synthesis. The concentrations of SnCl₄ solutions were appropriate for isomorphic substitution of 3, 6 and 12 % (wt.) Ti atoms by Sn atoms. The precursor solution together with the modifying reagent was diluted by water to reach pH = 0.5-2 and heated at 60-70 °C for 1 h. The reaction medium becomes cloudy and acquires a whitish hue during the heating. This indicates the formation of very small oxide particles. NaOH was used to increase the pH of solution. The formed particles were removed from the dispersed medium using a vacuum filter and washed from Na⁺ and Cl⁻ ions with distilled water and dried at a temperature of 120-140 °C. The obtained samples with different concentration of Sn atoms and standard were marked as 3Sn/TiO₂, 6Sn/TiO₂ and 12Sn/TiO₂, respectively. Non-doped titania sample was synthesized at the same conditions and was marked as a-TiO₂.

XRD analysis of studied samples has been carried out in the range of 10-80° using X-ray diffractometer with CuK α anode ($\lambda = 0.15406$ nm).

Morphology of Sn-doped TiO₂ particles was investigated by the transmission electron microscopy (TEM) using the JEM-2100F microscope (the accelerating voltage was 200 kV).

The textural and adsorption characteristics of the Sn-doped TiO₂ samples (the specific surface, pore volume, pore size distribution) were estimated from N₂ adsorption/desorption isotherms using surface area analyzer Quantachrome Autosorb Nova 2200e at 77 K. Before all measurements, the samples were degassed in vacuum for 24 h at 180 °C.

Infrared spectra of Sn-doped TiO₂ samples were registered on the SPECORD M80 spectrophotometer in the range of 4000-300 cm⁻¹. To record the spectrum, 4 mg of the sample was mixed with dry KBr in the ratio of 1:100 and crushed in a vibrating mill for 5 min. The prepared mixture was compressed to form trans-

parent pellets (20 × 5 mm²).

The elemental chemical composition of the Sn-doped TiO₂ samples was performed by energy-dispersive spectroscopy (EDS) using REMMA-102-02 Scanning Electron Microscope-Analyzer (JCS SELMI, Ukraine).

A capacitor system consisting of two blocking copper electrodes was used to record the conductive characteristics of the materials. The test sample is located between the electrodes. Impedance hodographs $Z'' = f(Z')$, where Z' and Z'' are the real and imaginary parts of the complex resistance of the system, respectively. They were obtained using amplitude-frequency analyzer Autolab/FRA-2 (Holland) in the frequency range of 10⁻²-10⁵ Hz. The amplitude of the sinusoidal voltage was 10 mV.

3. RESULTS AND DISCUSSION

3.1. Phase Composition and Structural Properties of Sn-doped TiO₂ Samples

The X-ray diffraction patterns of the undoped TiO₂ and doped 3Sn/TiO₂, 6Sn/TiO₂ and 12Sn/TiO₂ samples (Fig. 1) indicate their crystalline structure. The phase composition and structural characteristics of the samples are given in Table 1.

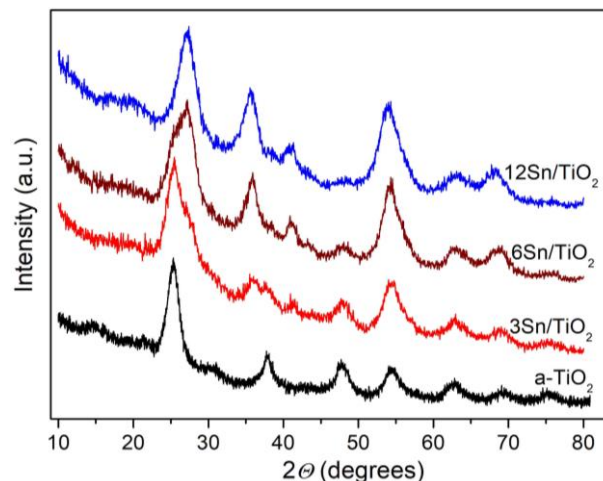


Fig. 1 – X-ray diffraction patterns of undoped TiO₂ and Sn-doped TiO₂ (3, 6, and 12 % (wt.) of Sn)

Table 1 – Phase composition and structural parameters of undoped TiO₂ and Sn-doped TiO₂ samples

Sample	Rutile			Anatase		
	Content, %	<i>a</i> , Å	<i>c</i> , Å	Content, %	<i>a</i> , Å	<i>c</i> , Å
a-TiO ₂	–	–	–	100	3.786	9.430
3Sn/TiO ₂	33.8 ± 1.24	4.5864 ± 0.0028	2.9729 ± 0.0031	66.2 ± 2.21	3.8142 ± 0.0023	9.3992 ± 0.0133
6Sn/TiO ₂	57.2 ± 1.65	4.6041 ± 0.0016	2.9883 ± 0.0015	42.8 ± 2.33	42.8 ± 2.33	9.4049 ± 0.0214
12Sn/TiO ₂	97.1 ± 2.52	4.6463 ± 0.0015	2.9971 ± 0.0013	2.9 ± 0.79	3.7569 ± 0.0048	9.4746 ± 0.0116

The undoped TiO₂ is single-phase and demonstrates an anatase structure. The doped samples consist of two phases: anatase and rutile. An increase in the content of Sn (IV) cations leads to an increase in the content of rutile. Thus, the samples 3Sn/TiO₂, 6Sn/TiO₂ and

12Sn/TiO₂ contain 33.8, 57.2 and 97.1 % (wt.) of rutile, respectively. These data indicate that the Sn atoms, intercalated in the titanium dioxide structure, act as promoters of the rutile formation.

The structural parameters of rutile depend more on

the dopant content. Fig. 2a demonstrates the increase in a and c lattice parameters of the rutile phase with increasing Sn content.

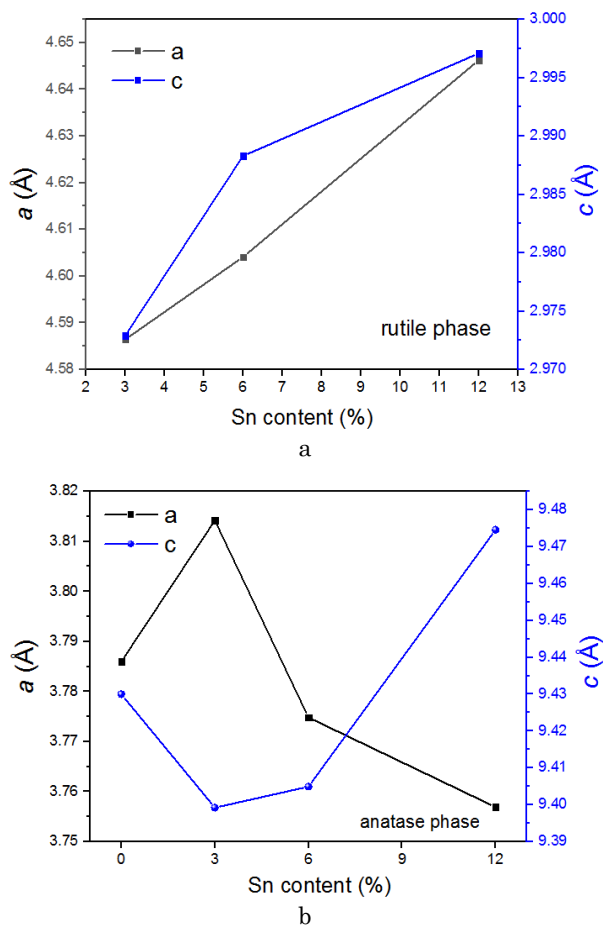


Fig. 2 – The dependence of structural parameters of doped TiO_2 samples versus Sn content: (a) lattice parameters of rutile phase; (b) lattice parameters of anatase phase

The main reason is the larger ionic radius of Sn (IV) cations (0.71 Å) in comparison with that of Ti (IV) ions (0.68 Å). The increase in Sn–O and Ti–O interatomic distances comparatively with anatase caused the nucleation of rutile crystal phases of titania. The nonlinear changes of anatase phase lattice parameters with increasing Sn content (Fig. 2b) can be explained by the influence of crystallites size variation [5].

3.2 TEM and EDS of Sn-doped TiO_2 Samples

The phase content of the 3Sn/ TiO_2 sample is about 66.2 % (wt.) of anatase and 33.8 % (wt.) of rutile. The observed rod-like shaped particles have a length in a range of 4-8 nm, thickness of about 0.8-1.0 nm and square cross-section corresponding to rutile phase [17]. Accordingly to TEM images, rod-shaped particles are surrounded by the spherical particles which most likely have the structure of anatase. The particle size of the anatase phase is in a range of 5-20 nm (Fig. 3a). The 6Sn/ TiO_2 sample consists of spherical anatase and rod-shaped rutile particles and also needle-like rutile particles with a length of 7-20 nm and diameter of about 0.6-0.8 nm. Thin needle-like rutile particles filled the

gaps between the associates formed by anatase particles (Fig. 3b). The 12Sn/ TiO_2 sample with rutile content of about 97 % (wt.) consists of needle-like particles mostly (Fig. 3c). The length of the needles is in a range of 7-120 nm, their diameter is close to 1 nm.

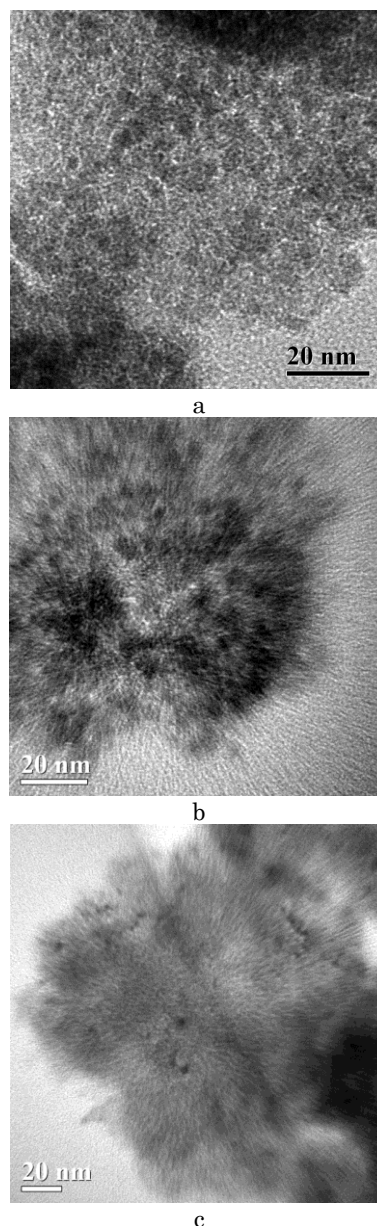


Fig. 3 – TEM images of Sn-doped titania samples: (a) 3Sn/ TiO_2 , (b) 6Sn/ TiO_2 , and (c) 12Sn/ TiO_2

The results of energy-dispersion spectroscopy showed that the elemental compositions of the doped TiO_2 samples correspond to the theoretically predicted (Table 2) and do not contain other impurities.

Table 2 – Elemental composition of Sn-doped TiO_2 samples

Sample	% (wt.)			Total
	Ti	O	Sn	
a- TiO_2	59.94	40.06	–	100
3Sn/ TiO_2	58.29	39.42	2.29	100
6Sn/ TiO_2	55.33	38.52	6.15	100
12Sn/ TiO_2	50.68	37.42	11.90	100

The Ti content decreases from 59.94 % for undoped TiO_2 to 50.68 % for the $12\text{Sn}/\text{TiO}_2$ sample with increasing Sn content. Only peaks of the chemical elements Ti, Sn and O are observed in the EDS spectra (Fig. 4).

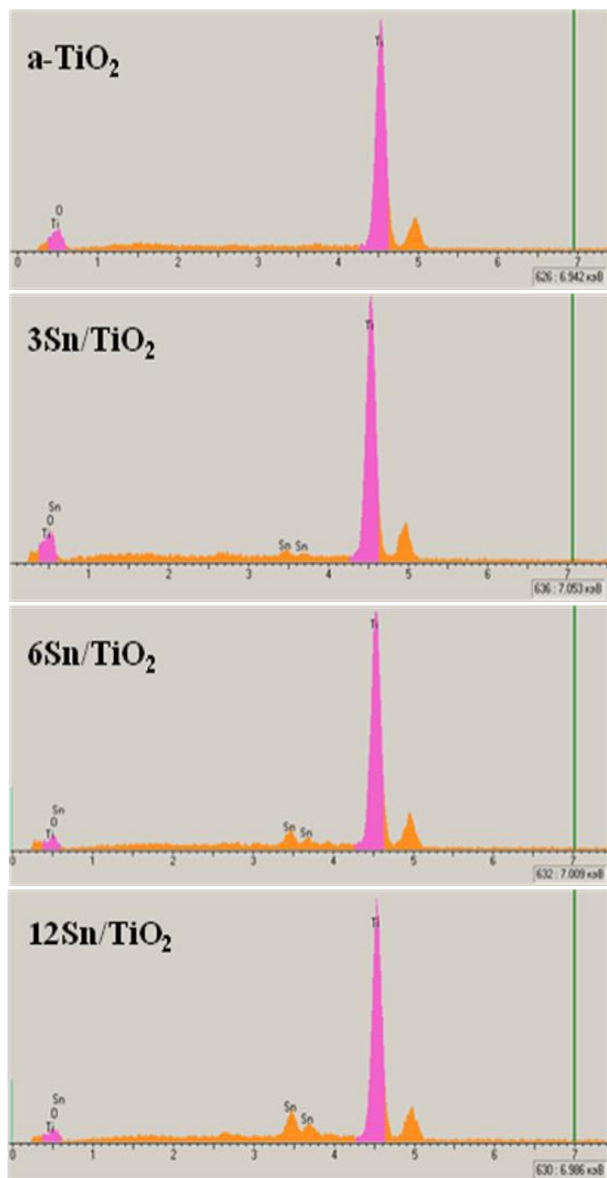


Fig. 4 – EDS spectra of Sn-doped titanium dioxide samples

3.3 Porous Structure of Sn-doped Titanium Dioxide Samples

The N_2 adsorption/desorption isotherms for Sn-doped and undoped TiO_2 samples are shown in Fig. 5. The textural characteristics (specific surface area, pore volume) of the studied samples, calculated from N_2 adsorption/desorption isotherms, are given in Table 3. The pore size distributions for Sn-doped and undoped TiO_2 samples are shown in Fig. 6.

The doping of titania with Sn (IV) cations leads to a significant increase in the specific surface area and pore volume of the modified samples compared to the undoped a- TiO_2 sample. The specific surface area S_{BET} of the undoped sample is about $239 \text{ m}^2/\text{g}$, while S_{BET} for $3\text{Sn}/\text{TiO}_2$ and $6\text{Sn}/\text{TiO}_2$ samples is about 281 and

$290 \text{ m}^2/\text{g}$, respectively. A characteristic feature of the Sn-doped titania is the presence of mesopores with the radius in a range of 1.0-2.5 nm. The volume of mesopores V_{meso} for $3\text{Sn}/\text{TiO}_2$ and $6\text{Sn}/\text{TiO}_2$ samples exceeds the volume of mesopores of undoped a- TiO_2 sample by 2.4-2.8 times. It is noteworthy that the specific surface area of the $12\text{Sn}/\text{TiO}_2$ sample is smaller compared to $3\text{Sn}/\text{TiO}_2$ and $6\text{Sn}/\text{TiO}_2$ samples and equals $205 \text{ m}^2/\text{g}$.

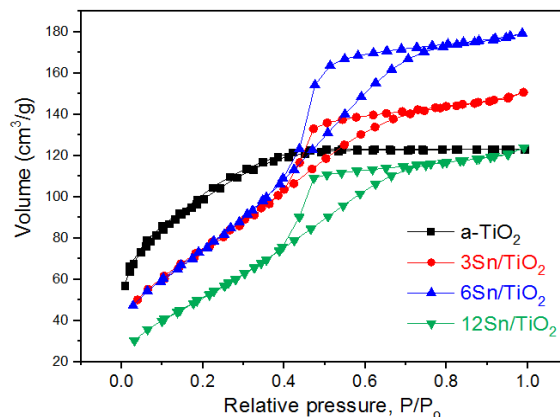


Fig. 5 – The N_2 adsorption/desorption isotherms for undoped and Sn-doped titania samples

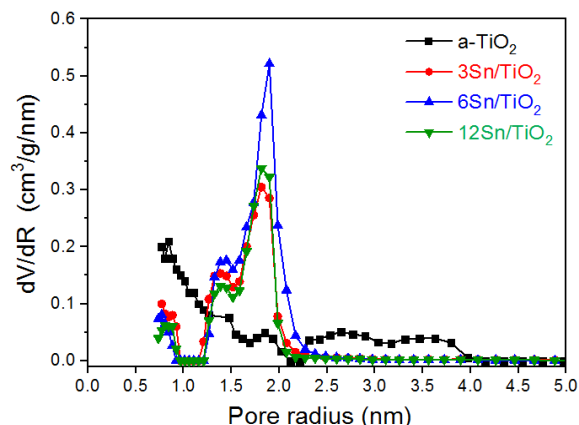


Fig. 6 – Pore size distribution for undoped and Sn-doped titania samples

Table 3 – Morphological characteristics of the studied samples

Sample	S_{BET} , m^2/g	S_{micro} , m^2/g	S_{meso} , m^2/g	V_p , cm^3/g	V_{micro} , cm^3/g	V_{meso} , cm^3/g
a- TiO_2	239	100	139	0.152	0.054	0.098
$3\text{Sn}/\text{TiO}_2$	281	–	281	0.233	–	0.233
$6\text{Sn}/\text{TiO}_2$	290	–	290	0.277	–	0.277
$12\text{Sn}/\text{TiO}_2$	205	–	205	0.192	–	0.192

3.4 IR-spectroscopy of Sn-doped TiO_2 Samples

IR-spectra of the undoped a- TiO_2 sample, as well as doped samples, are shown in Fig. 7. The degenerate vibrations E_u of TiO_6 octahedrons in the anatase structure of the a- TiO_2 sample are manifested by two bands at 548 cm^{-1} and 480 cm^{-1} [6]. The bands at 330 cm^{-1} and 730 cm^{-1} belong to symmetric vibrations A_u of octahedral sites [4, 5]. The presence of rutile phase in the $3\text{Sn}/\text{TiO}_2$ sample is confirmed by bands 430 cm^{-1} , 625 cm^{-1} (E_u vibrations) and 360 cm^{-1} , 750 cm^{-1} (A_u vibrations).

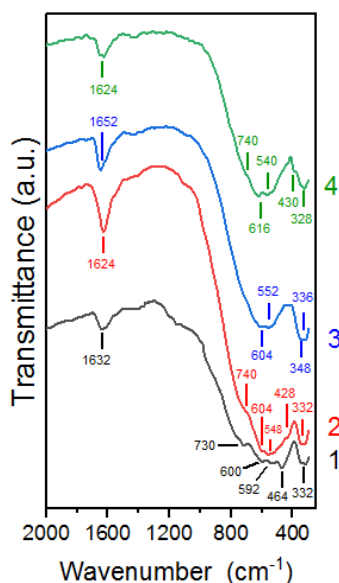


Fig. 7 – IR-spectra of Sn-doped titanium oxide samples: 1 – a-TiO₂; 2 – 3Sn/TiO₂; 3 – 6Sn/TiO₂; 4 – 12Sn/TiO₂

It is characteristic that the frequency characteristics of degenerate vibrations of the octahedrons change with increasing rutile content in 6Sn/TiO₂ and 12Sn/TiO₂ samples. Thus, the bands of this vibration mode are at 415 cm⁻¹ and 660 cm⁻¹ and the band of symmetrical vibrations is at 390 cm⁻¹ in the 12Sn/TiO₂ sample. The change in the frequency characteristics of the vibration modes of rutile is due to the increase in the geometric dimensions of the SnO₆ and TiO₆ octahedra with the rise of Sn (IV) cations. The band with the maximum absorption at 1630-1620 cm⁻¹ in the IR-spectra belongs to the deformation vibrations of water molecules adsorbed on the titania samples surface.

3.5 The Mechanism of Structure-forming Processes

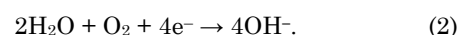
The substitution of Ti ions by Sn ions during the titania sol-gel synthesis leads to the nucleation of anatase/rutile mixture or rutile only phases with an especial particle morphology. The formation of rutile needle-like nanoparticles is caused by the presence of Sn(OH)₄·2H₂O species in the reaction medium which act as the centers of nucleation, growth and crystallization of rutile phase. Sn(OH)₄·2H₂O species are involved in the condensation process together with Ti(OH)₄·2H₂O species. The geometric parameters of the [SnO₆] coordination polyhedra formed at nucleation are close to the parameters of [TiO₆] polyhedra of the rutile phase. Thus, they take part in the formation of the titania structure and act as a template that determines the way of the crystallization process.

The electronegativity of Sn (χ_{Sn}) is equal to 1.8 and exceeds the value of the electronegativity of Ti ($\chi_{\text{Ti}} = 1.5$) [18], so Sn (IV) cations more actively attract OH⁻ anions. The greater attraction force of hydroxyl in the ≡SnOH group compared to the attraction force of hydroxyl in the ≡TiOH group makes the first group more acidic. This provides a high reaction activity of Sn(OH)₄·2H₂O species in the condensation process with Ti(OH)₄·2H₂O species.

The high dispersion degree of the doped samples is provided primarily by the fact that the formation of oxide particles takes place in an acidic environment (pH = 0.5-2.0). Under these conditions, the rate of nucleation centers formation exceeds the rate of their growth. The hydrolysis of Ti (IV) and Sn (IV) cations in an acidic reaction medium is due to the oxidation of Ti (III) cations during the heating of the precursor solution at a temperature of 70 °C:



This causes the reduction of water molecules with the participation of adsorbed oxygen molecules in the reaction:



In turn, OH⁻ anions are attached to the Ti (IV) and Sn (IV) cations and form Ti(OH)₄·2H₂O and Sn(OH)₄·2H₂O molecules. Their condensation leads to the formation and growth of particles with anatase/rutile or rutile crystalline structure.

3.6 Conductive Properties of Sn/TiO₂ Samples

The impedance hodographs of the studied materials are shown in Fig. 8.

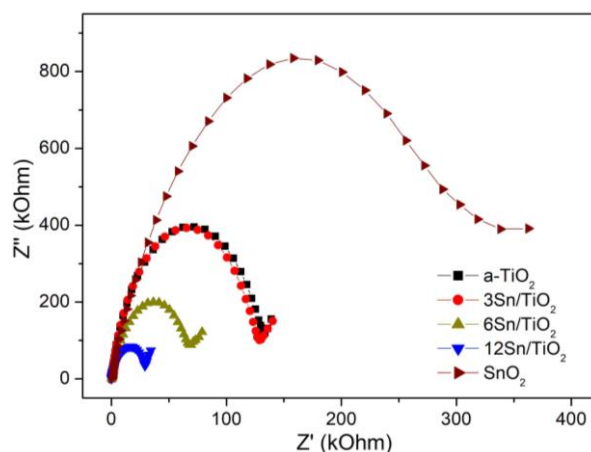


Fig. 8 – The impedance hodographs of the studied samples

They demonstrate that Sn doping of titanium dioxide leads to quantitative changes in the values of the real Z' and imaginary Z'' resistances. An increase in the Sn content leads to a decrease in the resistance of the studied materials compared to the undoped a-TiO₂ sample. The general view of impedance hodographs indicates the dominance of the capacitive component of the imaginary resistance over the inductive one. All the hodographs have the form of deformed semicircles in the high and medium frequency range. This indicates the scattering of charge carriers in both the volume of particles (grains) and the intergrain boundaries. The low-frequency section is a straight line inclined at an angle close to 45° to the true axis, which indicates the diffusion mechanism of conductivity in the studied materials.

The specific values of resistances, electrical conductivities and frequency dependences of the electrical parameters were calculated taking into account the geometric parameters of the samples:

$$\rho^* = \rho' - j\rho'', \quad (3)$$

$$\rho' = Z'A/d, \quad (4)$$

$$\rho'' = Z''A/d, \quad (5)$$

where A and d are the surface area of the electrode and the thickness of the sample, respectively. The total conductivity of materials was determined by the formula (6) [19]:

$$\sigma = \sqrt{(\sigma')^2 + (\sigma'')^2}, \quad (6)$$

where $\sigma' = \rho'/M$, $\sigma'' = \rho''/M$, $M = |Z^*|^2 (A/d)^2$, $Z^* = \sqrt{(Z')^2 + (Z'')^2}$.

The experimentally obtained frequency dependences of the conductivity $\sigma(\omega)$ (Fig. 9) are typical for semiconductors with percolation transport of current carriers (electrons) between localized electronic states. The obtained at room temperature dependences are characteristic of structurally disordered semiconductor systems. In particular, there is a gradual increase in the specific conductivity value in the low-frequency range and a sharp increase in its growth rate in the high-frequency part of the spectrum.

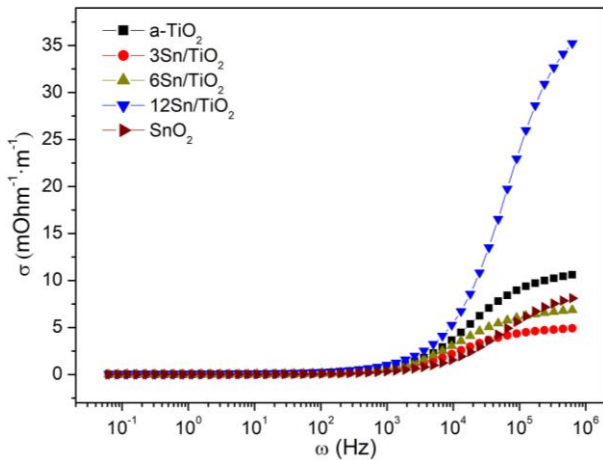


Fig. 9 – Frequency dependences of the total conductivity for the studied samples

The approximation of the $\sigma(\omega)$ dependences was carried out on the basis of the Jonscher equation [20] (the error did not exceed $\pm 5\%$) (Fig. 9):

$$\sigma(\omega) = \sigma_{dc} + A\omega^n, \quad (7)$$

where σ_{dc} is the frequency-independent conductivity in the DC mode; A is the characteristic parameter; n is a parameter that means a measure of interparticle interaction ($0 < n < 1$). The parameter n characterizes the deviation of the system from the properties

provided by the Debye model. The application of this approach involves the mechanisms of charge transfer due to non-Debye relaxation in solids: the generation-recombination processes involving localized states in the band gap, phonon-controlled jumps of electrons or ions in a disordered potential field, and polarization effects. The approximation results are presented in Table 4.

The results presented in Table 4 indicate that the substitution of 12 % (wt.) of Ti (IV) cations in titanium dioxide by Sn (IV) cations leads to an increase in the conductivity σ_{dc} by more than two times compared to the undoped a-TiO₂. The increase in the conductivity σ_{dc} is due to an increase in localized electronic states in the volume and on the surface of titania samples. The formation of localized states in the doped titania oxides is due to the higher electronegativity of Sn ions compared to the electronegativity of Ti ions.

Table 4 – The approximation of experimental data parameters to the Jonscher equation

Sample	σ_{dc} , mOhm ⁻¹ m ⁻¹	A , 10 ⁻⁶	n	R^2 , %
a-TiO ₂	0.021	5.3	0.71	99.84
3Sn/TiO ₂	0.015	6.3	0.63	99.63
6Sn/TiO ₂	0.024	10.1	0.61	99.67
12Sn/TiO ₂	0.057	10.1	0.65	99.73
SnO ₂	0.0058	8.2	0.58	99.64

4. CONCLUSIONS

The structure, morphology and conductive properties of Sn-doped TiO₂ samples have been investigated. The samples were obtained through sol-gel method using $[\text{Ti}(\text{OH})_2]_6^{3+} \cdot 3\text{Cl}^-$ as a precursor and tin tetrachloride as a modifying agent. It was shown that the isomorphous substitution of Sn (IV) ions in the titanium dioxide structure promotes the rutile phase formation. The reason of rutile nucleation is the elongation of interatomic distances Sn–O and Ti–O. The Sn/TiO₂ samples contain both anatase and rutile phases. An increase in the concentration of Sn ions doping leads to an enlargement of the rutile phase content (97.1 wt. %). All Sn-doped samples demonstrated mesoporous structure with the highest specific surface area of 290 m²/g, while undoped TiO₂ is characterized by the presence of micropores too. The IR-spectra confirmed the presence of rutile phase. The electrical conductivity of titania sample with the highest Sn content is more than twice higher compared to the undoped titania due to an increase in localized electronic states. This is conditioned by the higher electronegativity of Sn atoms compared to the electronegativity of Ti atoms.

ACKNOWLEDGEMENTS

The Ministry of Education and Science of Ukraine (project number 0120U102035) financially supported this research work.

REFERENCES

1. L.I. Halaoui, N.M. Abrams, T.E. Mallouk, *J. Phys. Chem. B.* **109**, 6334 (2005).
2. J.C. Yu, H.Y. Tang, J. Yu, H.C. Chan, L. Zhang, Y. Xie, H. Wang, S.P. Wong, *J. Photochem. Photobiol. A Chem.* **153**, 211 (2002).
3. M. Paulose, O.K. Varghese, G.K. Mor, C.A. Grimes, K.G. Ong, *Nanotechnology* **17**, 398 (2006).
4. I. Mironyuk, T. Tatarchuk, H. Vasylyeva, M. Naushad, I. Mykytyn, *J. Environ. Chem. Eng.* **7**, 103430 (2019).
5. I. Mironyuk, T. Tatarchuk, H. Vasylyeva, V.M. Gun'ko, I. Mykytyn, *J. Mol. Liq.* **282**, 587 (2019).
6. I. Mironyuk, T. Tatarchuk, M. Naushad, H. Vasylyeva, I. Mykytyn, *J. Mol. Liq.* **285**, 742 (2019).
7. T. Tatarchuk, A. Shyichuk, I. Mironyuk, M. Naushad, *J. Mol. Liq.* **293**, 111563 (2019).
8. A. Fujishima, K. Honda, *Nature* **238**, 37 (1972).
9. N. Danyliuk, J. Tomaszewska, T. Tatarchuk, *J. Mol. Liq.* **309**, 113077 (2020).
10. A. Olivo, E. Ghedini, M. Signoreto, M. Compagnoni, I. Rossetti, *Energies* **10**, 1 (2017).
11. P. Pookmanee, S. Phanichphant, *J. Ceram. Process. Res.* **10**, 167 (2009).
12. K.M. Reddy, D. Guin, S.V. Manorama, A.R. Reddy, *J. Mater. Res.* **19**, 2567 (2004).
13. B. Qi, L. Wu, Y. Zhang, Q. Zeng, J. Zhi, *J. Colloid Interface Sci.* **345**, 181 (2010).
14. D.A.H. Hanaor, C.C. Sorrell, *J. Mater. Sci.* **46**, 855 (2011).
15. M.I. Franch, J. Peral, X. Domenech, J.A. Ayllon, *Chem. Commun.* **14**, 1851 (2005).
16. R. Khayyam Nekouei, F. Pahlevani, M. Mayyas, S. Maroufi, V. Sahajwalla, *J. Environ. Chem. Eng.* **7**, 103133 (2019).
17. V. Kotsyubynsky, I. Myronyuk, V. Chelyadyn, A. Hrubciak, V. Moklyak, S. Fedorchenko, *J. Nano Res.* **50**, 32 (2017).
18. Y. Zhang, *Inorg. Chem.* **21**, 3886 (1982).
19. M.H. Abdullah, A.N. Yusoff, *J. Alloy. Compd.* **233**, 129 (1996).
20. A.K. Jonscher, *Universal Relaxation Law: A Sequel to Dielectric Relaxation in Solids* (Dielectrics Press, Chelsea, 1996).

Структура, морфологія та електропровідні властивості Sn-легованого TiO₂

І.Ф. Миронюк, Т.Р. Татарчук, В.О. Коцюбинський, В.І. Мандзюк, Х.О. Савка, І.М. Микитин

Прикарпатський національний університет імені Василя Стефаника, вул. Шевченка, 57,
76018 Івано-Франківськ, Україна

У роботі досліджено вплив легування Sn на структуру та морфологію Sn-легованих зразків TiO₂. Легований діоксид титану отримувався золь-гель методом з використанням аквакомплексу [Ti(OH)₆]³⁺·3Cl⁻ як прекурсору титану і SnCl₄ як модифікатора. Структура і морфологія зразків досліджувалися методами X-променевої дифрактометрії, ТЕМ аналізу, низькотемпературної порометрії, ІЧ та енергодисперсійної спектроскопії. Провідність Sn-легованих зразків TiO₂ вивчалася методом імпедансної спектроскопії. Встановлено, що Sn-леговані зразки діоксиду титану містять кристалічні фази анатазу і рутилу. Співвідношення анатаз/рутил залежить від вмісту Sn: збільшення вмісту Sn(IV) від 3 до 12 % (ваг.) зумовлює збільшення вмісту рутилу від 33,8 до 97,1 % (ваг.). Ріст вмісту Sn також призводить до зменшення параметра кристалічної ґратки *a* та збільшення параметра *c*. ТЕМ-методом виявлено наявність стрижневидних і голковидних частинок рутилу в Sn-легованих зразках TiO₂. Величина питомої поверхні для зразка 6Sn/TiO₂ становить 290 м²/г. Усі зразки Sn-легованого діоксиду титану є мезопористими. Механізми структуроутворюючих процесів пояснюються присутністю в реакційному середовищі молекул Sn(OH)₄·2H₂O, які діють як центри нуклеації, росту та кристалізації для наночастинок рутилу. Збільшення вмісту Sn зумовлює також зменшення питомого опору досліджуваних матеріалів порівняно із нелегованим зразком діоксиду титану.

Ключові слова: Діоксид титану, Рутил, Анатаз, Оксид олова(IV), Питома електропровідність.